Supporting Information

Atmospheric Chemical Reaction Mechanism and Kinetics of 1,2-Bis(2,4,6-tribromophenoxy)ethane Initiated by ·OH Radicals: A Computational Study†

Qi Yu,[a] Hong-Bin Xie,*[a] Tianchi Li,[a] Fangfang Ma,[a] Zihao Fu,[a] Zhongyu Wang,[a] Chao Li,[b] Zhiqiang Fu,[a] Deming Xia[a] and Jingwen Chen[a]

Contents

Details for the test of DFT methods

Since there is no experimental data for the reaction of BTBPE + ·OH and calculations of higher-

† Electronic Supplementary Information (ESI) available: details of methods and rate calculation, Table S1, S2, Figure S1-S3. See DOI: xxxxx

[a] *Key Laboratory of Industrial Ecology and Environmental Engineering (Ministry of Education), School of Environmental Science and Technology, Dalian University of Technology, Dalian 116024, China*

[b] *State Environmental Protection Key Laboratory of Wetland Ecology and Vegetation Restoration, School of Environment, Northeast Normal University, Changchun 130117, China*

level theoretical approaches such CCSD(T) exceeds the computational capabilities at present, we evaluated the performance of the selected DFT method on the reaction of BTBPE + ·OH by comparing the calculated reaction rate constants of small molecules having similar reactivity to the active groups of BTBPE, toward ·OH with corresponding available experimental values. In view of molecular structure, bromophenyl group and ethyl group of BTBPE are the reactive groups toward ·OH. Here, the bromophenyl and methyl ether were selected as testing small molecules. Previous study found the PBE1PBE functional has a good performance for predicting the barrier height of addition pathway (the most favorable one) for the reaction of ·OH with aromatics.[1] Thus, PBE1PBE functional was firstly selected for testing systems. The k_{OH} of C_6H_5Br + ·OH is calculated to be 1.3×10^{-12} cm^3 $molecule^{-1}$ s^{-1} based on the calculated energetic information at PBE1PBE/6-311++G(3df,2pd)//PBE1PBE/6-31+G(d,p) (PBE1PBE/6-31+G(d,p) optimized geometries, followed by PBE1PBE/6-311++G(3df,2pd) single point energy calculation) level. The calculated k_{OH} is consistent well with the experimental value ($(9.37 \pm 2.04) \times 10^{-13}$ cm^3 $molecule^{-1}$ s^{-1}),[2] indicating that PBE1PBE method is reliable to predict the k_{OH} value of addition pathways for BTBPE + ·OH. However, the calculated k_{OH} value (6.5×10^{-11} cm^3 $molecule^{-1}$ s^{-1}) of CH_3OCH_3 + ·OH is around one order higher than experimental value ($(2.67\pm0.07) \times 10^{-12}$ cm^3 $molecule^{-1}$ s^{-1}).[3] Alternatively, we test another DFT method (M062X/6-311++G(3df,2pd)//M062X/6-31+G(d,p)) to predict the H-abstraction barrier.[4] At this level, the calculated k_{OH} of CH_3OCH_3 + ·OH is 2.2×10^{-12} cm^3 $molecule^{-1}$ s^{-1}, matching the experimental data well.[3] Therefore, in this study, both functionals PBE1PBE and M062X were used. The M062X was selected to study H-abstraction process in the OH initiated reactions and PBE1PBE for all other processes.

Details for the barrierless reaction rate constant calculation

The rate constants for the barrierless entrance reaction of IM7-1+O_2 was calculated by the restricted Gorin model based on the experimental rate constant (2.1×10^{-12} cm^3 $molecule^{-1}$ s^{-1} at 298 K) of its similar

system CH_3OCH_2+O_2.[5] The Hindered Gorin Model implemented in the Mutilwell code[6] has the capability to automatically find the hindrance parameters for the Hindered Gorin transition state according to basic input parameters such as the center of mass distance.[7-13]

The long-range transition state theory was used to calculate the barrierless entrance reaction of BTBPE+·OH because there is no related experimental data. The values for the employed polarizabilities and the first ionisation potentials are 339.68 $bohr^3$, 8.25 eV and 8.32 $bohr^3$, 13.02 eV for BTBPE and ·OH, respectively, in the long-range transition state theory calculations. The data for ·OH stemmed from the NIST database,[14] and those for BTBPE came from calculations. The polarizabilities were calculated at BLYP/def2-QZVPD, which has been proven to be able to accurately predict the polarizability of molecules.[15] First ionisation potentials were calculated at the PBE1PBE/6-311++G(3df,2pd)//PBE1PBE/6-31+G(d,p) level, which is verified by comparing the first ionisation potentials for HCl between experiment (12.74 eV) and calculation(12.67 eV).

Table S1. The configuration and relative Gibbs free energies (to global minimum) of 5 BTBPE conformers.

	Configuration	Relative free energy (kcal mol^{-1})
1	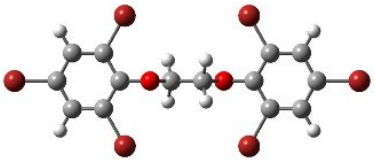	0
2	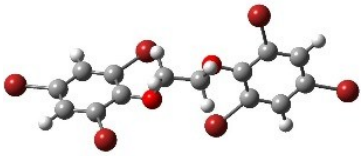	3.66
3	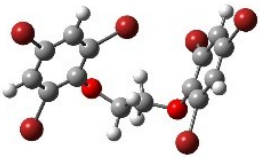	6.19
4	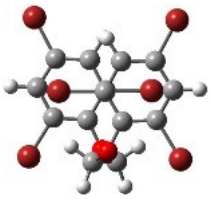	8.69
5	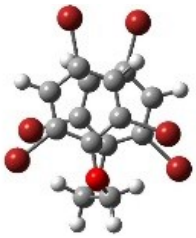	9.38

Table S2. Calculated activation free energy values ($\Delta G^{\ddagger}$), activation enthalpy values ($\Delta H^{\ddagger}$) and product ($\Delta S^{\ddagger}T$) of activation entropy ($\Delta S^{\ddagger}$) and temperature (T) for the reaction BTBPE + ·OH (Unit is in kcal mol^{-1}) at 298 K.

Pathways	Species[a]	$\Delta G^{\ddagger}$	$\Delta H^{\ddagger}$	$\Delta S^{\ddagger}T$[b]
Addition	IM1	9.7	0.2	-9.5
	IM1’	9.7	0.2	-9.5
	IM2	13.9	3.6	-10.3
	IM2’	13.9	3.6	-10.3
	IM6	13.9	3.6	-10.3
	IM6’	13.4	3.4	-10.0
	IM3	7.6	-1.4	-9.0
	IM3’	7.6	-1.4	-9.0
	IM5	7.6	-1.4	-9.0
	IM5’	7.6	-1.4	-9.0
	IM4	10.6	2.6	-8.0
	IM4’	10.5	2.6	-7.8
H-abstraction	IM7-1	8.7	-1.7	-10.4
	IM7-2	8.7	-1.7	-10.4
	IM7’-1	8.7	-1.7	-10.4
	IM7’-2	8.7	-1.7	-10.4
	IM3-H	14.4	5.3	-9.1
	IM3’-H	14.4	5.3	-9.1
	IM5-H	14.4	5.3	-9.1
	IM5’-H	14.4	5.3	-9.1

[a] The species correspond to the reaction pathways showed in Figure 2. [b] $\Delta S^{\ddagger}T = \Delta H - \Delta G$, $T = 298$ K.

Table S3. Calculated k (s^{-1} for unimolecular rate constants and cm^3 $molecule^{-1}$ s^{-1} for bimolecular rate constants) and pseudo-first order rate constants k' (s^{-1}) for the subsequent reactions of IM3 and IM7-1.

Reaction pathways[a]	k[b]	k'[c]
IM7-1 → P7 + P8[d]	3.3×10^{4}	-
IM7-1 + O_2 → IM14[e]	2.2×10^{-12}	1.1×10^{7}
IM7-1 + NO[e]	$\sim10^{-12}$	$\sim10^{-2}$
IM3 → P1+Br[d]	3.6×10^{-18}	-
IM3 → P2[d]	4.7×10^{-8}	-
IM3 + O_2 → P9[e]	2.2×10^{-21}	1.1×10^{-2}
IM3 + O_2 → P10[e]	4.6×10^{-27}	2.3×10^{-8}
IM3 + O_2 → P11[e]	0	0
IM3 + O_2 → P12[e]	0	0
IM3 + O_2 → P13[e]	3.9×10^{-24}	1.9×10^{-5}
IM3 + O_2 → P14[e]	0	0
IM3 + O_2 → P15[e]	6.5×10^{-25}	3.2×10^{-6}
IM3 + O_2 → P16[e]	0	0
IM3 + O_2 → P17[e]	1.8×10^{-26}	8.9×10^{-8}
IM3 + O_2 → P18[e]	6.0×10^{-25}	3.0×10^{-6}
IM3 + O_2 → P19[e]	0	0
IM3 + O_2 → P20[e]	0	0
IM3 + O_2 → P21[e]	1.3×10^{-22}	6.3×10^{-4}
IM3 + NO[e]	$\sim10^{-14}$	$\sim10^{-4}$

[a] Correspond to the reaction pathways showed in Figure 4 and 5. [b] Calculated at 298K, 1 atm. [c] Bimolecular rate constants multiplied by concentration of O_2 or NO. [d] Unimolecular reaction pathways. [e] Bimolecular reaction pathways.

Table S4. Predicted Daphnia Magna LC50 values (48h, mg L^{-1}) for BTBPE and OH-BTBPE via VEGA in silico platform.

	BTBPE	OH-BTBPE
EPA 1.0.7[a]	0.0097	0.016
DEMETRA 1.0.4[b]	0.0255	3.04

[a] EPA version 1.0.7: QSAR model for Daphnia Magna LC50 (48h), based on multiple linear regression. The model extends the original model implemented in the T.E.S.T. software. The original model was developed by US EPA inside the T.E.S.T. software and can be freely accessd at http://www.epa.gov/nrmrl/std/cppb/qsar/.

[b] DEMETRA version 1.0.4: Acute toxicity for Water Flea (Daphnia Magna) for pesticides: LC50 48-hours exposure. Built as a Hybrid Model upon two ANNs and a single PLS. Based on the model built for DEMETRA project (http://www.demetra-tox.net).

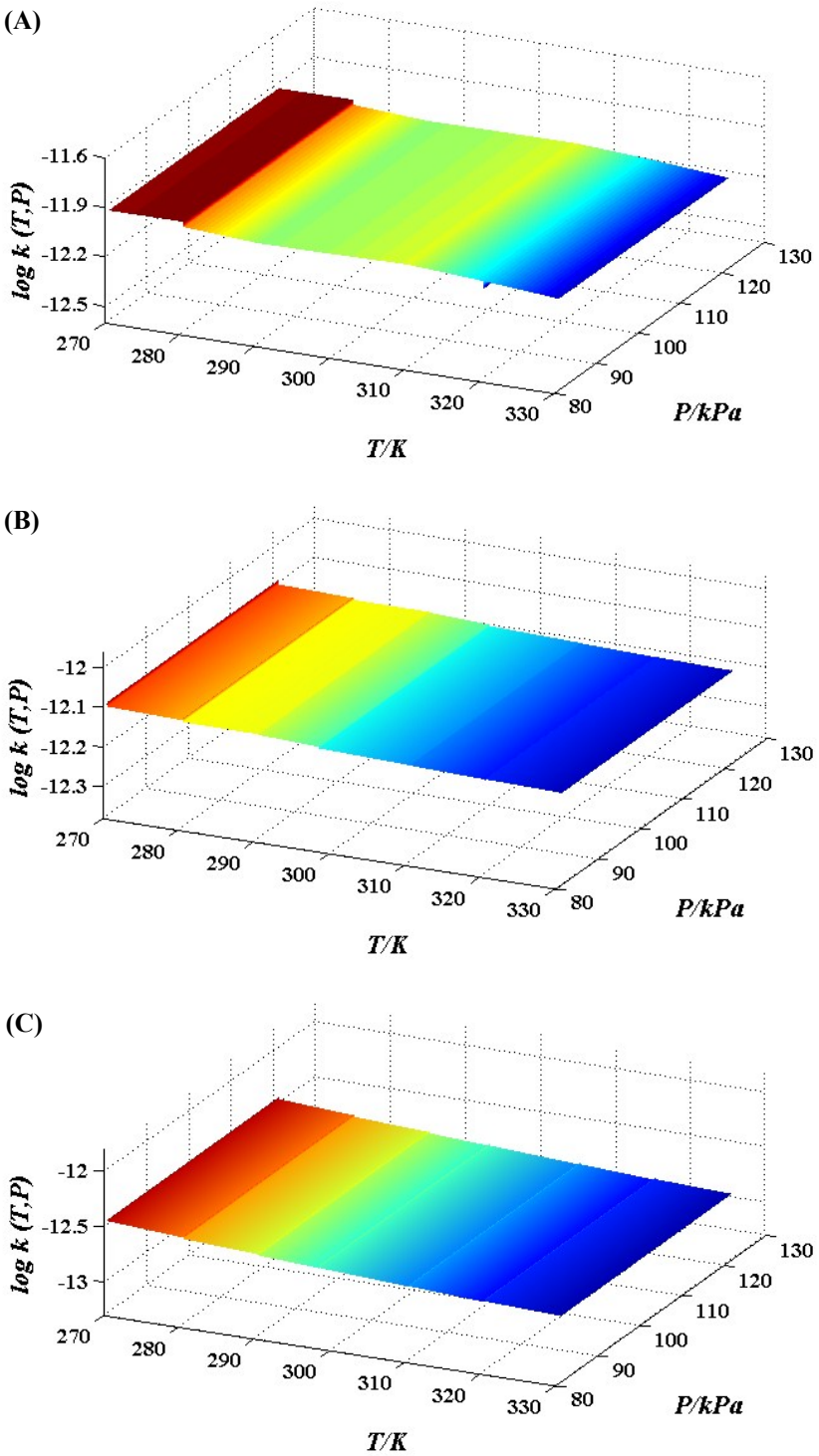

Figure S1. Calculated rate constants $k_{(T,P)}$ (cm^3 $molecule^{-1}$ s^{-1}) as a function of temperature (T) and pressure (P) for the overall reaction pathways (A) and two most favorable pathways forming intermediates (B: IM3+IM3'+IM5+IM5', C: IM7-1+IM7'-1+IM7-2+IM7'-2).

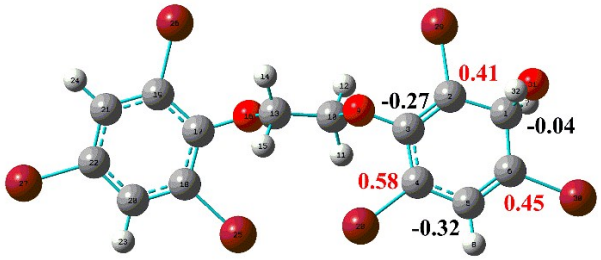

Figure S2. Mulliken atomic spin densities for the C-atoms of part of IM3 adduct. High spin density values are highlighted in red.

References

1 G. P. Wood, A. Sreedhara, J. M. Moore, B. L. Trout. *J. Phys. Chem. A,* 2014, **118,** 2667-82.

2 Y. Nakano, M. Kawasaki, D. A. Ponomarev, M. D. Hurley, T. J. Wallington. *Chem. Phys. Lett.,* 2002, **353,** 77-83.

3 A. Bonard, V. Daële, A. Jeanlouis Delfau, C. Vovelle. *J. Phys. Chem. A,* 2002, **106,** 4384-4389.

4 Y. Zhao, D. Truhlar. *Theor. Chem. Acc.,* 2008, **120,** 215-241.

5 M.E. Jenkin, G.D. Hayman, T.J. Wallington, M.D. Hurley, J.C. Ball, O.J. Nielsen, T. Ellermann. *J. Phys. Chem.,* 1993, **97,** 11712–11723.

6 MultiWell-2014 Software, 2014, designed and maintained by John R. Barker with contributors Nicholas F. Ortiz, Jack M. Preses, Lawrence L. Lohr, Andrea Maranzana, Philip J. Stimac, T. Lam Nguyen, and T. J. Dhilip Kumar; University of Michigan, Ann Arbor, MI; http://aoss.engin.umich.edu/multiwell/.

7 D. M. Golden. *J. Phys. Chem. A,* 2007, **111,** 6772-6780.

8 D. M. Golden. *J. Phys. Chem. A,* 2006, **110,** 2940-2943.

9 D. M. Golden. *Int. J. Chem. Kinet.,* 2005, **37,** 625–632.

10 D. M. Golden, J. R. Barker, L. L. Lohr. *J. Phys. Chem. A,* 2003, **107,** 11057-11071

11 D. M. Golden, G. P. Smith. *J. Phys. Chem. A,* 2000, **104,** 3991-3997.

12 R. Patrick, and D. M. Golden. *Int. J. Chem. Kinet.,* 1983, **15,** 1189–1227.

13 G. P. Smith, D. M. Golden. *Int. J. Chem. Kinet.,* 1978, **10,** 489-501.

14 NIST Computational Chemistry Comparison and Benchmark Database. NIST Standard Reference Database Number 101, R. D. Johnson III, Release 16a, August 2013. http://cccbdb.nist.gov/.

15 D. Rappoporta, F. Furche. *J. Chem. Phys.,* 2010, **133,** 134105-134111.